MATEMATIKA, MJIAM, Volume 41, Number 2, 193–211

Sakiadis Flow with Thermal Radiation and Richardson Number via Inclined Stretching Plate

Nur Hazirah Adilla Norzawary[2], Nurul Fatin Najim Johan[1], Siti Khuzaimah Soid[1*], Farizza Haniem Sohut[3], Amirah Mohamad Sahar[1], Mohd Rijal Ilias[1] and Umair Khan[4,5]

[1]School of Mathematical Sciences, College of Computing, Informatics, and Mathematics, Universiti Teknologi MARA, Malaysia
[2]Institute for Mathematical Research, Universiti Putra Malaysia, 43400, Selangor, Malaysia
[3]Department of Mathematical Sciences, Universiti Kebangsaan Malaysia, Malaysia
[4]Department of Mathematics, Faculty of Science, Sakarya University, Serdivan, Sakarya, 54050, Türkiye
[5]Department of Mechanics and Mathematics, Western Caspian University, Baku, 1001, Azerbaijan
[*]Corresponding author: khuzaimah@tmsk.uitm.edu.my

Article history
Received: 17 October 2024
Received in revised form: 26 March 2025
Accepted: 14 May 2025
Published online: 1 August 2025

Abstract This study aims to elucidate a steady two-dimensional laminar mixed convection boundary layer over an inclined stretching plate immersed in an incompressible viscous fluid. The governing partial differential equations (PDEs) are first reduced to ordinary differential equations (ODEs) using a similarity transformation, before being solved numerically using MATLAB software, which is based on the boundary value problem fourth order (bvp4c) method. The effects of the radiation parameter, angle of the plate, Richardson number, and the Prandtl number on the heat transfer and fluid flow characteristics are obtained and discussed. The impacts of flow constraints on the velocity profile, temperature profile, heat transfer rate and skin friction coefficients are presented in tables and figures. The observation indicates that the rate of heat transfer at the surface rises with increases in the Richardson number, and inclination of plate angle but it diminishes as the radiation parameter increases. Meanwhile, the drag force experiences a decrease with an increase in radiation and the inclination of the plate angle. However, it demonstrates an increase with the rise values of Richardson number and Prandtl number. This leads to enhanced buoyancy-driven flow effects, ultimately resulting in a reduced skin friction along the surface Moreover, a further analysis using Computational Fluid Dynamics (CFD) simulation is applied to solve the governing equations of flow in interesting applications, enhancing the understanding of boundary layer flow.

Keywords Radiation, Mixed convection, Richardson number, Inclined plate, Stretching, Sakiadis flow.

Mathematics Subject Classification 76N20, 93A30.

1 Introduction

Sakiadis [1] pioneered the investigation of boundary layer behaviour on continuous solid surfaces, leading to what is now known as Sakiadis flow. In his research, he observed that the boundary layer originates at the slot and progresses in the same direction as the surface motion. The fluid velocity in the x-direction at surface's solid equals the velocity of the surface itself. Moving away from the surface, the fluid's x-direction velocity gradually diminishes to zero. Concurrently, the y-direction velocity of the fluid changes from zero at the surface to a finite value at the boundary layer's edge. Essentially, Sakiadis flow characterizes the behavior of a boundary layer where the fluid is stationary, and the solid surface is in motion. A numerical comparison between Sakiadis and Blasius flows further highlights the distinct characteristics of Sakiadis flow, particularly in terms of velocity profiles and boundary layer thickness [2].

Viscous and incompressible fluid flow in a laminar boundary layer via moving plate at constant speed has been widely studied. Cortell [3] looked into fluid flow and heat transfer via stretching plate, considering factors like magnetic fields, viscoelastic fluids, and surfaces stretched by different forces, with suction/injection. Grubka and Bobba [4] studied flow via linearly stretching surface, while Soid and Ishak [5] extended this by including the radiation effects on steady flow via such plates in a viscous fluid. In real-world scenarios, many factors, especially radiation, must be considered when analysing fluid flow and heat transfer.

Manufacturing processes such as hot rolling, extrusion, melt-spinning, and wire drawing commonly involve flow via stretching surface. Soid and Ishak [5] highlighted the significant role of thermal radiation in high-temperature processes, noting that it cannot be overlooked. Solar energy stands out as a highly promising renewable resource, particularly as local energy reserves become depleted. Ghasemi and Hatami [6] pointed out that despite its slightly higher costs, solar energy is widely favoured for its environmental benefits and protective features. Solar radiation can produce heat for manufacturing processes, while thermal radiation plays a crucial role in heat transfer in high-temperature industries such as nuclear power plants, gas turbines, and thermal energy storage. Studies on radiation effects have been carried out by Dehsara *et al.* [7] Hayat *et al.* [8], Noor *et al.* [9], Izani *et al.* [10] and Mishra and Samantara [11].

2D laminar mixed convective flow via vertical flat plate is a key model often used in the literature as a basic example (Siddiqa and Hossain [12]). It's important to analyse various heat transfer methods on surfaces with high temperatures. One such mechanism involves the fluid absorbing, emitting, and scattering radiation, which allows for rapid heat exchange. Understanding heat and flow behaviour is critical to ensuring the final product meets quality standards. Many studies have focused on heat and fluid flow over stretching sheets, considering both Newtonian and non-Newtonian fluids [13–19].

Recent studies have expanded this focus to include complex factors such as thermal radiation, magnetic fields, and hybrid nanofluids, providing deeper insights into the heat transfer mechanisms involved. For instance, Balamurugan and Kumar [20] investigated the influence of quadratic convection in transient magnetohydrodynamic (MHD) combined convection over a stretching sheet, incorporating thermal radiation effects. Similarly, Alzu'bi *et al.* [21]conducted a numerical study on Casson mixed convection transport by ternary hybrid nanofluids over a vertical stretching sheet, considering Newtonian heating conditions. These studies underscore the importance of integrating various physical phenomena to accurately model and

analyze heat and fluid flow over stretching sheets.

Heat transfer refers to the exchange of energy due to temperature differences, while mass transfer involves the movement of a liquid mass within fluid flow, seen in processes like absorption, evaporation, and drying [22]. Mixed convection combines free convection, driven by buoyancy (represented by the Richardson number), together with forced convection, common in industrial processes [23]. Al-Sumaily *et al.* [24] note that most research has focused on either forced or natural convection, with less attention given to the combined effects of both. However, the interaction of mixed convection and heat radiation is significant.

Mandal *et al.* [22] observed that temperature and concentration vary near the plate's edge but remain constant further away. The inclination angle of the stretching plate causes the boundary layer thickness to decrease. Researchers like Alabdulhadi *et al.* [25], Hamad *et al.* [26], and Malik *et al.* [27] have studied steady, incompressible flow over inclined, stretching sheets to explore mass and heat transfer.

Computational Fluid Dynamics (CFD) is a branch of fluid mechanics that applies numerical methods and computational algorithms to solve and analyze fluid flow issues. It simulates how liquids and gases interact with surfaces, providing a valuable tool for predicting flow patterns, pressure, temperature, and concentration in a wide range of applications. CFD models rely on equations such as the Navier-Stokes equations to describe the motion of fluids. With advancements in computational power, CFD is now a widely used tool for design optimization, reducing the need for physical prototypes, and enhancing efficiency in multiple industries such as in the food industry [28] and Neurosurgery [29]. Dobhal and Gupta [30] evaluates different RANS turbulence models in CFD analysis for boundary layer flow via flat plate, using ANSYS Fluent 19.1. They concluded that model selection is critical for accurate simulation. It provides guidelines for selecting turbulence models based on mesh resolution and y+ values, highlighting the importance of different models for different boundary layer regions. Some other studies related to CFD are Mahdavi *et al.*, [31], Alhamid and Al-Obaidi [32] and Algaidy and El Shrif [33].

Researchers have been intrigued by the study of mixed convection boundary layer flow because it closely resembles real-world scenarios, accounting for gravity and temperature differences between the fluid and the plate. This makes the results similar to natural phenomena. This study will focus on flow of Sakiadis, thermal radiation, and number of Richardson via inclined stretching plate employing boundary value problem method (bpv4c) in MATLAB. It builds on Soid and Ishak's [5] previous research by adding the mixed convection parameter. The study explores how different plate angles affect fluid flow and heat transfer.

The inclusion of the mixed convection effect is significant because it enhances the accuracy of heat and mass transfer predictions, particularly in high-temperature manufacturing processes where buoyancy forces play a crucial role. Understanding how convection influences boundary layer development provides deeper insights into optimizing thermal management in industrial applications. Additionally, integrating CFD in this research allows for a comprehensive analysis of fluid dynamics by providing numerical simulations that complement theoretical models. CFD simulations offer visual and quantitative validation of flow behavior, aiding in the refinement of mathematical models and ensuring more precise predictions. The findings are expected to be valuable for Newtonian-based analyses of stretching plates and useful for engineers and researchers in industries like manufacturing, where optimizing heat transfer and fluid flow is essential for efficiency and product quality.

2 Mathematical Model

The study examines steady, 2D mixed convection boundary layer flows via inclined plate that stretches linearly and is submerged in an incompressible viscous fluid, as illustrated in Figure 1. The plate stretches at a constant positive velocity, denoted as $U_w = ax$. The ambient temperature T_∞ and the surface temperature T_w, are both assumed to be constant, with $T_w > T_\infty$. Here, g represents gravitational acceleration and Ω is the plate's angle.

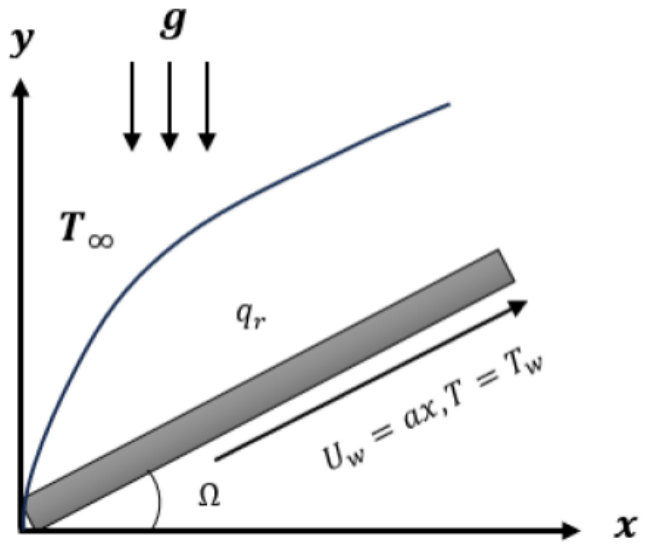

Figure 1: Physical model

The governing equations and the boundary conditions as following [5]:

$$\frac{\partial u}{\partial x} + \frac{\partial v}{\partial y} = 0 \tag{1}$$

$$u\frac{\partial u}{\partial x} + v\frac{\partial u}{\partial y} = v\frac{\partial^2 u}{\partial y^2} + g\beta\left(T - T_\infty\right)\sin\Omega \tag{2}$$

$$u\frac{\partial T}{\partial x} + v\frac{\partial T}{\partial y} = \alpha\frac{\partial^2 T}{\partial y^2} - \frac{1}{\rho c_p}\frac{\partial q_r}{\partial y} \tag{3}$$

subject to conditions of

$$\begin{aligned} v = 0, u = U, T = T_w \quad \text{at} \quad y = 0, \\ u \to 0, T \to T_\infty \quad \text{as} \quad y \to \infty \end{aligned} \tag{4}$$

u and v is the velocity component in the x- and y-direction, respectively, υ represents kinematic viscosity, T is temperature of the fluid, α is the thermal diffusivity, $\rho$is the fluid density, C_p and is the specific heat at constant pressure.

The radiative heat flux,q_r is defined using the Rosseland approximation, expressed as:

$$q_r = \frac{4\sigma}{3K}\frac{\partial T^4}{\partial y} \tag{5}$$

where K is the Rosseland mean absorption coefficient and σ is the Stefan-Bolzman constant. It is important to note that T is often expressed as a linear function of temperature as the flow's temperature difference is minimal.

$$T^4 \approx T_\infty^4 + (T - T_\infty)\, 4T_\infty^3 = 4T_\infty^3 T - 3T_\infty^4 \tag{6}$$

By applying (5) and (6) to (3), we gain

$$u\frac{\partial T}{\partial x} + v\frac{\partial T}{\partial y} = \alpha\left(\frac{\partial^2 T}{\partial y^2} + N\frac{\partial^2 T}{\partial y^2}\right) \tag{7}$$

The similarity variables were introduced,

$$\eta = \left(\frac{a}{\upsilon}\right)^{1/2} y, \psi = (\upsilon a)^{1/2} x f(\eta), \theta(\eta) = \frac{T - T_\infty}{T_w - T_\infty} \tag{8}$$

where η is the similarity variable and ψ is the stream function defined as $U = \partial\psi/\partial y$ and $v = -\partial\psi/\partial x$ which satisfied the continuity Eq. (1).

Using the similarity transformation variables, the PDEs are converted into ODEs as shown below:

$$f'(\eta)^2 - f(\eta)f''(\eta) - f'''(\eta) - \mathrm{Ri}\,\theta(\eta)\sin\Omega = 0 \tag{9}$$

$$\frac{1}{\mathrm{Pr}}(1+N)\theta''(\eta) - f(\eta)\theta'(\eta) = 0 \tag{10}$$

The conditions (4) are as follows:

$$\begin{aligned} f(0) = 0, f'(0) = 1, \theta(0) = 1 \quad \text{at} \quad \eta = 0 \\ f'(\eta) \to 0, \theta(\eta) \to 0 \quad \text{at} \quad \eta \to \infty \end{aligned} \tag{11}$$

where $Ri = Gr_x/Re_x^2 (= \text{const.})$ the Richardson number, where Gr_x is number of Grashof and Re_x is number of Reynolds, N is the radiation parameter and Pr is number of Prandtl, described as

$$Gr_x = \frac{g\beta\,(T_w - T_\infty)\,x^3}{v^2}, \quad \mathrm{Re}_x = \frac{U_w x}{v}, \quad N = \frac{16\sigma T_\infty^3}{3Kk}, \quad \mathrm{Pr} = \frac{v}{\alpha}. \tag{12}$$

The physical parameters, namely the skin friction coefficient C_f and local Nusselt number Nu_x are presented as follows [5]:

$$C_f = \frac{2\mu}{\rho U_w^2}\left(\frac{\partial u}{\partial y}\right)_{y=0}, \quad Nu_x = -\frac{xk}{k(T_w - T_\infty)}\left(\frac{\partial T}{\partial y}\right)_{y=0} \tag{13}$$

with μ and k are dynamic viscosity and thermal conductivity respectively. Using Eqs. (8) and (13) yields

$$\frac{1}{2}C_f Re_x^{1/2} = f''(0), \quad Nu_x Re_x^{-1/2} = -\theta'(0). \tag{14}$$

3 Results and Discussion

3.1 Detailed Evaluation of Results

Nonlinear ODEs Eq. (9-10) and conditions (11) are numerically solved utilizing boundary value problem solver (bvp4c) in MATLAB. This research takes into account the values of $N = 0, 0.5, 1, 5, 10, Ri = 1, 3, 5, 7, 10$ and $\Omega = 0, \frac{\pi}{6} \frac{\pi}{2}$, while Prandtl number is set to be constant, $Pr = 7$. $Pr = 7$ was chosen because it corresponds to water at standard conditions, making the study relevant to many industrial applications involving heat transfer in liquids. Additionally, previous studies [5] on boundary layer flow have commonly used this value, allowing for validation and comparison of results.

Table 1 shows the comparison values of the $-\theta'(0)$ for varies values of Pr and N with the absence of Ω and Ri which shows a favorable agreement with those obtained by Soid and Ishak [5]. In addition, Table 2 demonstrates the numerical values of skin friction coefficient $f''(0)$ and Nusselt number $-\theta'(0)$ of varies parameters when $Pr = 7$. The values of $f''(0)$ and $-\theta'(0)$ are increases as Ω, N and Ri increase. However, the values of $-\theta'(0)$ decreases only when $N$is increased. Furthermore, for the $\Omega = 0$ case, an increase in values of N causes no changes to the values of $f''(0)$ and for the increase of Ri, both $f''(0)$ and $-\theta'(0)$ also, the values remain the same

Table 1: $-\theta'(0)$ for varies of Pr and N for Ω=Ri=0

$-\theta' = (0)$			
Pr	N	Soid and Ishak [5]	Present (bvp4c)
0.7	0	0.4539	0.45391666
	0.5	0.3364	0.33639327
	1	0.2688	0.26903220
	5	0.1051	0.10506184
	10	0.0599	0.05996650
1	0	0.5820	0.58197671
	0.5	0.4383	0.43827498
	1	0.3544	0.35445628
	5	0.1444	0.14436909
	10	0.0836	0.08362953
3	0	1.1652	1.16524595
	0.5	0.9114	0.91135768
	1	0.7603	0.76028951
	5	0.3544	0.35443745
	10	0.2195	0.21953644
7	0	1.8954	1.89540326
	0.5	1.5075	1.50746165
	1	1.2762	1.27615604
	5	0.6454	0.64536813
	10	0.4238	0.42375763

Table 2: Values of $f''(0)$ and $-\theta'(0)$ for some values of Ω and N values when $Pr = 7$

Ω	N	Ri	$f''(0)$	$-\theta'(0)$
0	0	1	-1.00000000	1.89540326
	0.5		-1.00000000	1.50746165
	1		-1.00000000	1.27615604
	5		-1.00000000	0.64536813
	10		-1.00000000	0.42375763
		1	-1.00000000	0.42375763
		3	-1.00000000	0.64536813
		5	-1.00000000	0.64536813
		7	-1.00000000	0.64536813
		10	-1.00000000	0.64536813
$\pi/2$	0		-0.75106735	1.93032573
	0.5		-0.70648260	1.54967027
	1		-0.67146994	1.32436507
	5		-0.51623756	0.72307190
	10		-0.42479667	0.51932328
		1	-0.42479667	0.51932328
		3	0.29145063	0.80675966
		5	1.00882531	0.86283876
		7	1.67469001	0.90670973
		10	2.60931423	0.95977339

The velocity $f''(\eta)$ and temperature profile $\theta(\eta)$ are represented graphically in Figures 2 to 11 for varies N, Ri and when Pr = 7. A consistent $f''(\eta)$ is depicted in Figure 2 because the value of N, Pr and Ri do not affect the flow at the horizontal plate ($\Omega = 0$). As indicated in Eq. (9), it is anticipated because Pr and N are not present, while the Richardson number Ri is influenced by the angle of the plate. Therefore, only a single valid curve was generated, and the boundary layer thickness remained unchanged. Figure 3 illustrates an increase in response to rising N values. Importantly, the increase in the temperature profile results in a thicker thermal boundary layer. This is expected because the addition of radiation provides extra heat near the plate. This increase enables the fluid to move more rapidly, resulting in higher temperature and velocity within the boundary layer region.

In Figures 4 and 6, $f'(\eta)$ shows that as N increases, the thickness of the boundary layer also increases. The Richardson number Ri is important in Equation (9) because it influences the flow around plates that are positioned either vertically or at an angle. In Figures 5 and 7, the temperature profile rises with increasing N values. Additionally,$f'; (0)$ on the plate increases, while $-\theta; (0)$ decreases as N rises, as indicated in Table 2. This occurs because, as N increases, the fluid temperature rises, making the temperature difference between the plate's surface and the free stream nearly the same, which slows down $-\theta; (0)$ up to thermodynamic equilibrium is achieved. This effect is particularly important when the plate is inclined. Furthermore, the two coefficients change when comparing vertical and horizontal plate placements.

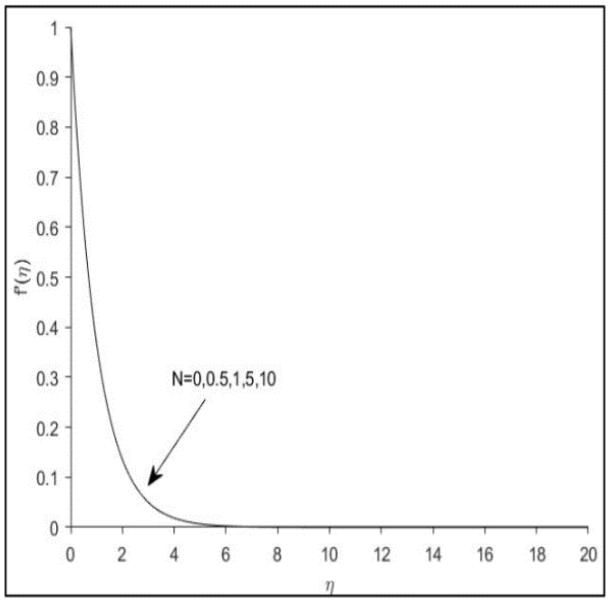

Figure 2: $f'(\eta)$ for varies N values when Pr=7, Ri=1 and $\Omega = 0$

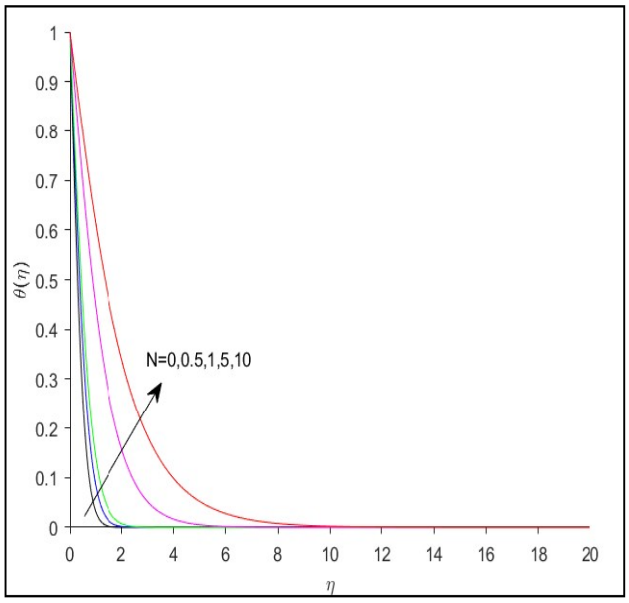

Figure 3: $\theta(\eta)$ for varies N values when Pr=7, Ri=1 and $\Omega = 0$

Figures 8 to 11 illustrate the $f'(\eta)$ and $\theta(\eta)$ for distinct Ri at $\Omega = \pi/6$ and $\Omega = \pi/2$ respectively. From Table 2, an increase in Ri, shows $f''(0)$ tends to increase due to enhanced buoyancy effects.$-\theta'(0)$ also increases as the Ri goes up. This is because stronger convection from buoyancy forces helps move more heat from the surface to the fluid. This trend is especially significant when the plate is inclined. Figures 8 and 10 indicate that for higher Ri, the velocity is considerably greater. Ri is the ratio between the Gr_x and Re_x . Since Re_xhas an inversely proportional relationship with fluid velocity $f'(0)$, the fluid velocity increases as Ri changes. However, when η approaches 3, the behaviour shifts, leading to a rapid decrease in the boundary layer thickness, approaching zero faster than other cases. Meanwhile, the boundary layer thickness in the temperature profile, as shown in Figures 9 and 11, decreases with increasing Ri. This means that higher Ri values result in a quicker drop in the plate's temperature. Consequently, Ri is essential for maintaining fluid flow stability and enhancing the heat transfer rate within the boundary layer.

As the angle increases, both $f''(0)$ and $-\theta'(0)$ rise, as shown in Table 2. Meanwhile, Figure 12 shows that the thickness of the boundary layer in $f'(\eta)$ increases, while Figure 13 displays the opposite trend in $\theta(\eta)$, where the thickness decreases. Additionally, when the plate is vertical ($\Omega = \pi/2$), the fluid flows faster because the buoyancy force decreases with increased plate inclination. Thus, as Ω increases, the momentum boundary layer thickness increases, whereas the thermal boundary layer thicknesses decrease.

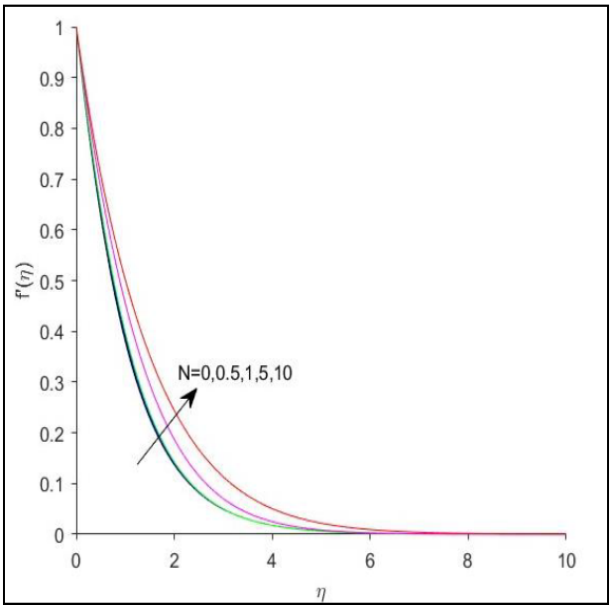

Figure 4: $f'(\eta)$ for varies N values when Pr=7, Ri=1 and $\Omega = \pi/6$

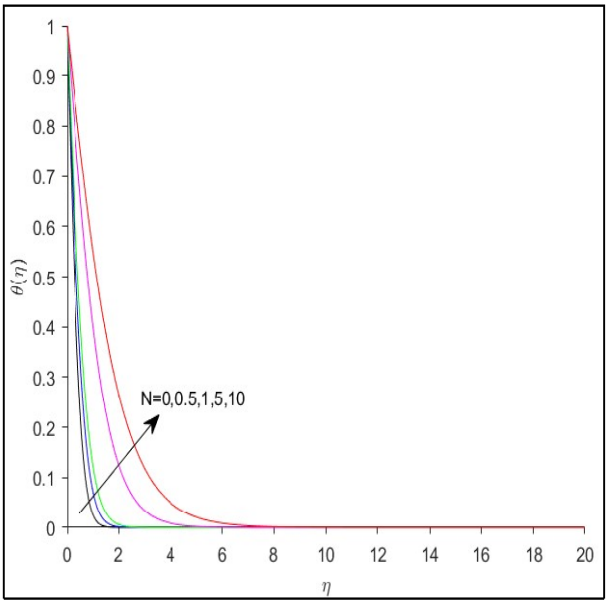

Figure 5: $\theta(\eta)$ for varies N values when Pr=7, Ri=1 and $\Omega = \pi/6$

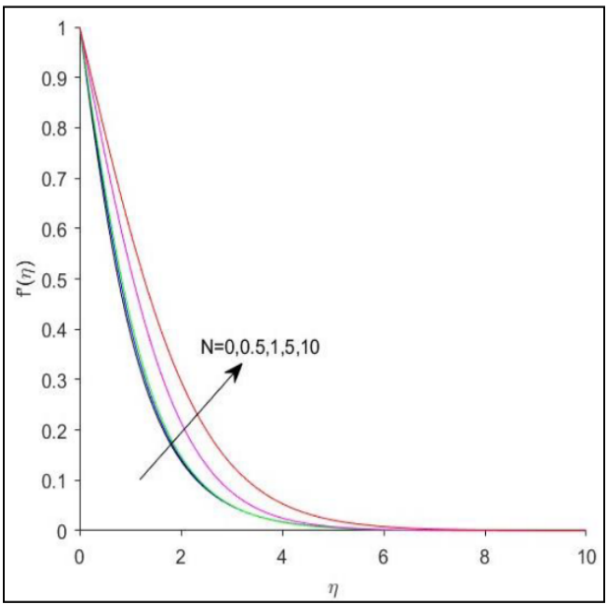

Figure 6: $f'(\eta)$ for varies N values when Pr=7, Ri=1 and $\Omega = \pi/2$

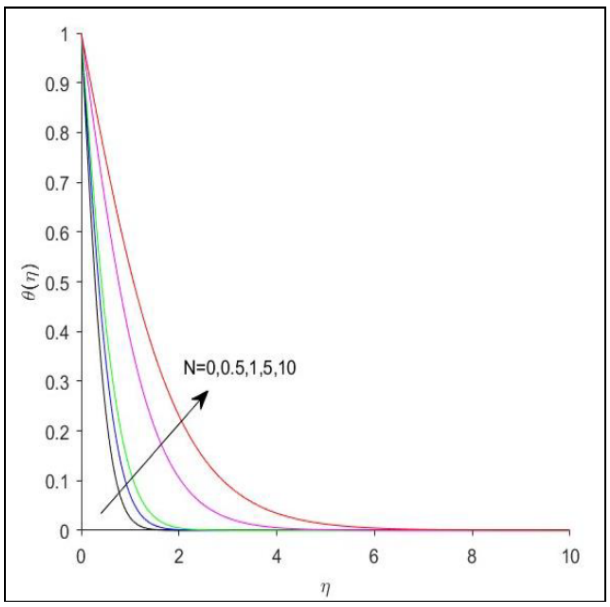

Figure 7: $\theta(\eta)$ for varies N values when Pr=7, Ri=1 and $\Omega = \pi/2$

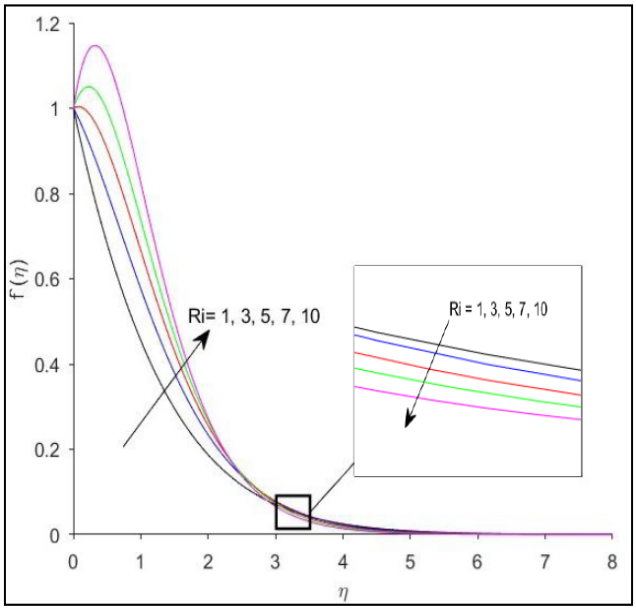

Figure 8: $f'(\eta)$ for varies Ri values when Pr=7, $N = 5$ and $\Omega = \pi/6$

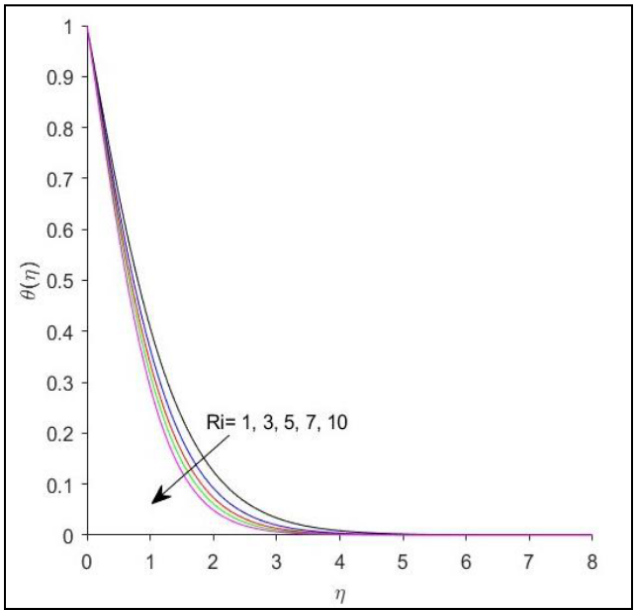

Figure 9: $\theta(\eta)$ for varies Ri values when Pr=7, $N = 5$ and $\Omega = \pi/6$

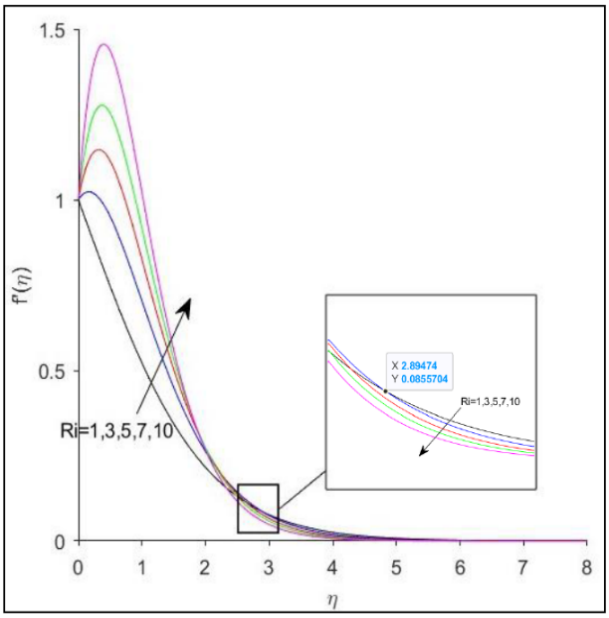

Figure 10: $f'(\eta)$ for varies Ri values when Pr=7, $N = 5$ and $\Omega = \pi/2$

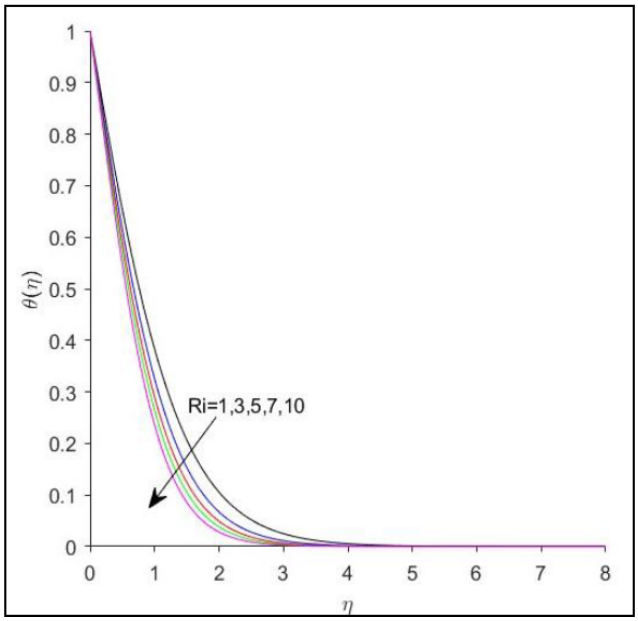

Figure 11: $\theta(\eta)$ for varies Ri values when Pr=7, $N = 5$ and $\Omega = \pi/2$

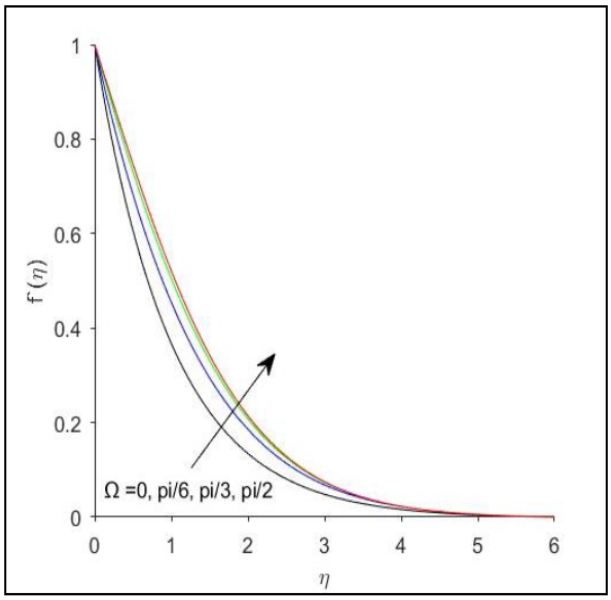

Figure 12: $f'(\eta)$ for varies Ω values when Pr=7,$N = 5$ and Ri=1

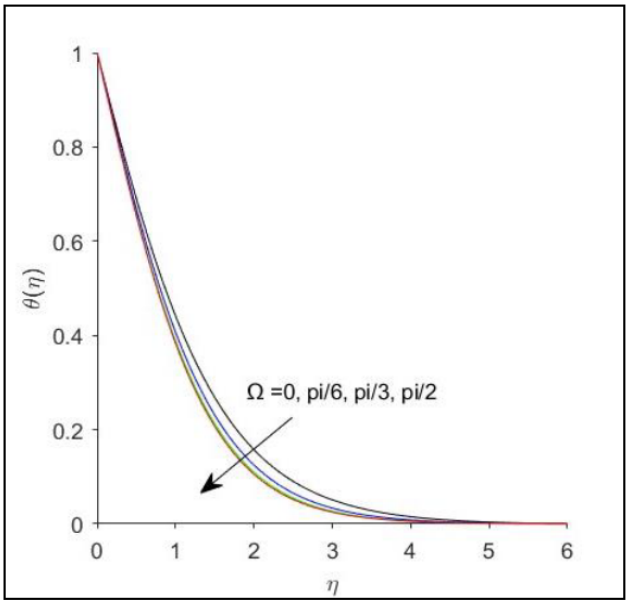

Figure 13: $\theta(\eta)$ for varies Ω values when Pr=7,$N = 5$ and Ri=1

3.2 Computational Fluid Dynamics (CFD)

Boundary layer problems can be solved numerically using various methods, including the method of Runge-Kutta, finite difference method, boundary value problem techniques, and CFD simulations. Klazly and Bognar [34] investigated airflow over a flat plate to examine hydrodynamic and thermal boundary layers through CFD simulations, utilizing Ansys Fluent R18.1 to solve the governing flow equations. Their results showed excellent agreement between analytical and numerical solutions, with a maximum error of less than 6.19%.

In computational fluid dynamics, numerical methods are used to analyse and solve fluid flow problems with the CFD software package Ansys Fluent. For this case study, the plate is inclined ($\Omega = \pi/6$), and radiation and mixed convection are taken into account. The CFD process involves creating the geometry, generating the mesh, setting physical parameters, and solving the problem.

Figure 14 illustrates the flow configuration of the computational domain. The plate is 1 meter long parallel the x-axis, and the heights of boundaries AB and CD are 0.1 meters across the y-axis. Fluid flows via the plate surface from boundary AB, the inlet, to boundary CD, the outlet. Boundary BC represents the plate surface, while boundary AD is characterized as symmetry. Figure 15 displays the geometry model for the flow configuration, created via DesignModeler, as the plate is tilted at a specified angle ($\Omega = \pi/6$).

The next step in this simulation involves creating a computational mesh. In order to analyse fluid flow accurately, the flow area is divided into smaller element (quadrilaterals or triangles for 2D models). In this study, Fluent is used for mesh generation. The inlet and outlet are divided into 50 sections employing a specific division method with a bias factor of 50 to increase detail near the critical plate area for better accuracy. The sides, symmetry, and plate are also divided into 120 sections each.

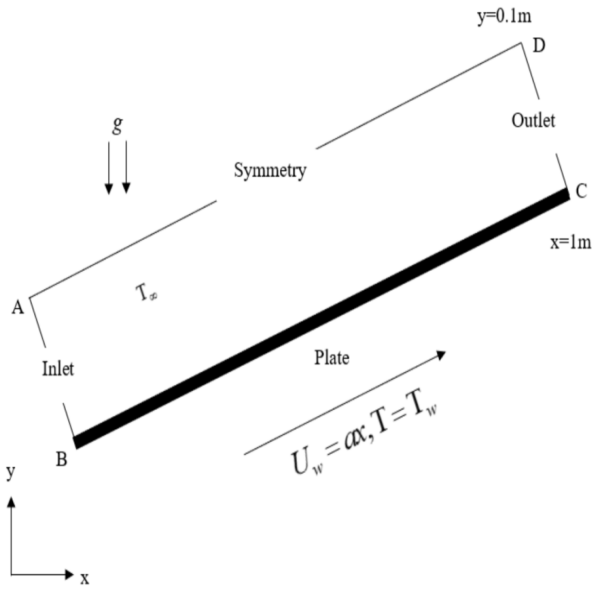

Figure 14: The flow configuration

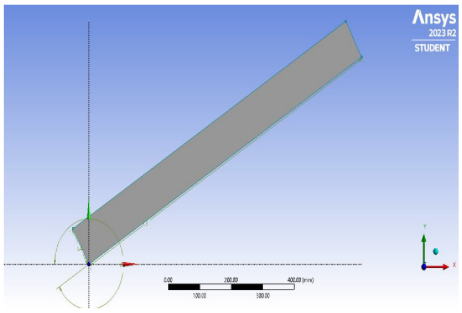

Figure 15: Geometry model

Figures 16 and 17 show the results of the mesh generation. Figure 16 displays the mesh in DesignModeler, while Figure 17 shows the fluid flow and plate surface in Ansys Fluent. The blue arrow indicates fluid entering through the inlet and moving over the plate, while the red arrow shows the fluid exiting at the outlet. Fluid flow is strongest near the plate surface.

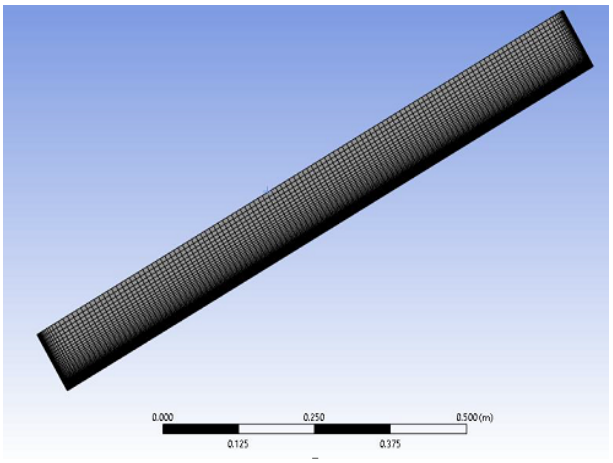

Figure 16: Generated Meshing in Design Modeler

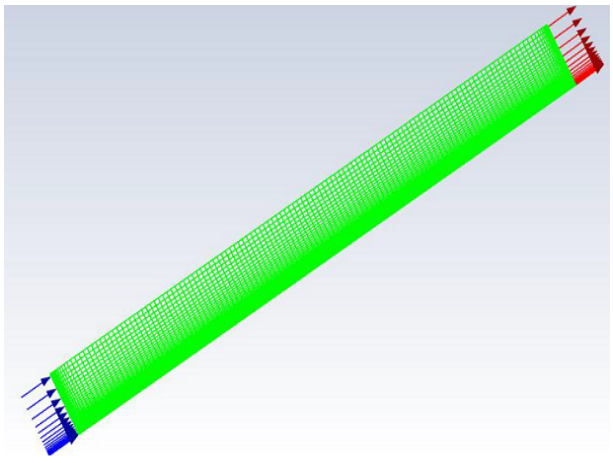

Figure 17: Generated Meshing in Fluent solver with the direction of fluid flow

For the next stage, the fluid flow and thermal boundary conditions for the model are specified based on the parameters from Ansys Fluent. Boundary AB (velocity inlet), has both horizontal and vertical velocities set to zero. Boundary CD (pressure outlet), having static pressure equal to ambient pressure, and other flow values derived from the interior. The plate BC is represented as a wall, with the horizontal velocity maintained as constant and the vertical velocity equal to zero. Boundary AD is a symmetry line, meaning there are no vertical velocity changes.

The fluid properties are provided by the Fluent solver and listed in Table 3, together with the boundary conditions in Table 4.

Table 3: The physical properties

Name	Fluid properties	Value
Density	ρ	998.2 (kg/m^3)
Dynamic Viscosity	μ	1.003×10^{-3}(kg/ms)
Thermal conductivity of the fluid	k	0.0242

Table 4: Boundary conditions

Name	Fluid properties	Value
Length	x	1
Ambient fluid velocity	U_∞	0
Velocity fluid on the surface	U_w	1
Ambient fluid temperature	T_∞	300
Wall temperature	T_w	400
Prandtl number	Pr	6.99091

Finally, the Navier-Stokes equations, and energy equation that includes N, Ri and Ω setup, were resolved to obtain the solution numerically. The simulation used a laminar solver with a 2nd-order upwind method for discretizing the equations. The inlet velocity was set to zero, while the wall moved at 1 meter per second. Calculations were done with high precision, and the solution's progress was tracked using a residual monitor with a set convergence criterion of 10^{-6}.

Table 5 shows that there is only a slight difference in $f''(0)$ and $-\theta'(0)$ values between the numerical solutions from MATLAB and the CFD software. Table 5 shows that $f''(0)$ is slightly negative in MATLAB (-0.6522) but positive in the CFD software (0.6615), indicating different directions of the friction force. A negative value means the flow is experiencing adverse pressure gradients, potentially leading to boundary layer separation or flow reversal. In contrast, a positive value suggests favourable pressure gradients, promoting smooth flow along the surface. $-\theta'(0)$ values obtained from MATLAB and CFD are in a good agreement with 98%. These numbers represent how fast heat is transferred to or from the surface. The small differences may be due to mesh resolution, or convergence criteria used in each simulation.

Table 5: The comparison value of $f''(0)$ and $-\theta'(0)$ between MATLAB and CFD

	$f''(0)$	$-\theta'(0)$
MATLAB	-0.65221258	0.37996613
CFD	0.661521	0.37214224

Figures 18 and Figure 19 illustrate the velocity contour and velocity direction. The colour scale ranges from blue (lowest velocity) to red (highest velocity), with green, yellow, and orange showing increasing speeds. In Figure 18, the velocity is highest at the surface and incrementally decreases until it becomes uniform in the inviscid region above the boundary layer. This contour shows the velocity distribution across the plate. Figure 19 displayed velocity vectors across the plate. The fluid near the plate surface has the highest velocity due to the wall's movement, but this decreases gradually because of friction, eventually reaching zero at the free stream. This underscores the significance of accounting for boundary layer behavior and shear stress by means of examining fluid flow via moving wall in CFD simulations.

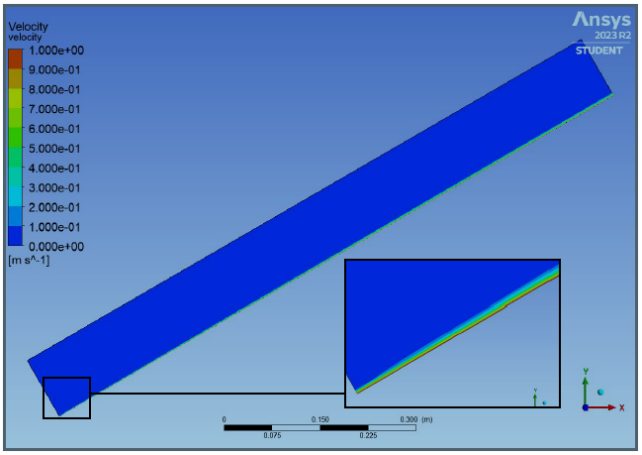

Figure 18: Velocity contour

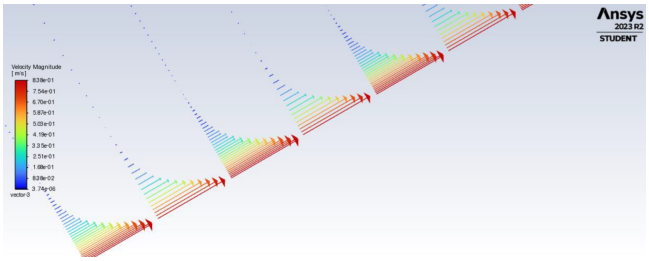

Figure 19: Velocity direction

Another key finding, illustrated in Figure 20, is the pressure contour, which could not be calculated using MATLAB. Though it's a bit hard to see, the contour is most noticeable at the inlet's leading edge, shown by a light blue colour indicating low pressure. As the flow progresses towards the outlet, the pressure gradually increases, transitioning to a red colour, which represents higher pressure. This pressure distribution is important in simulations with an inclined moving plate, as it provides valuable insights into fluid flow dynamics and boundary layer behaviour. Pressure gradients are essential in determining how the fluid accelerates or decelerates along the plate, impacting both the stability of the boundary layer and the potential for flow separation.

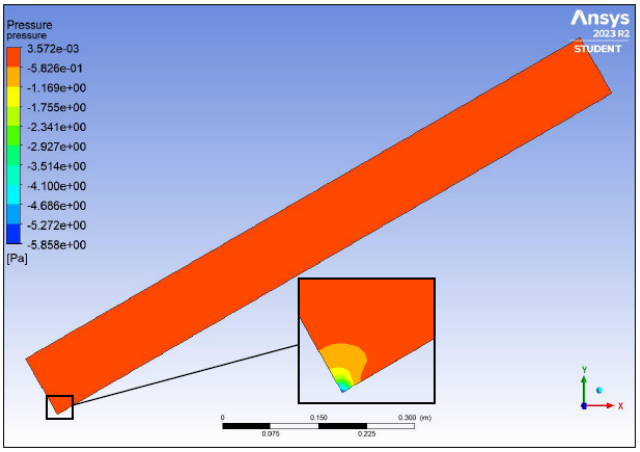

Figure 20: Pressure contour

Additionally, understanding the pressure distribution is vital for optimizing engineering designs, as it helps minimize drag and maximize heat transfer efficiency. Figure 21 shows the temperature distribution across inclined flat plate, with a colour gradient from blue (lowest) to red (highest). In regions of low pressure, the increased fluid velocity can enhance convective heat transfer, while higher pressure regions may slow down the flow, reducing the heat transfer rate. At the plate's surface, there is a thin boundary layer where the temperature peaks at 400K, shown in red. As the distance from the surface increases, the temperature progressively decreases, stabilizing at a uniform value (blue) of 300K, which corresponds to the free stream temperature in the inviscid region near the outlet. These temperature variations are primarily attributed to the fluid's thermal conductivity, facilitated by heat convection amid the plate and the fluid. By accurately mapping the pressure contours, this study provides a deeper understanding of how pressure variations affect both fluid flow and thermal management, making it highly relevant for design improvements in fields such as aerospace and manufacturing.

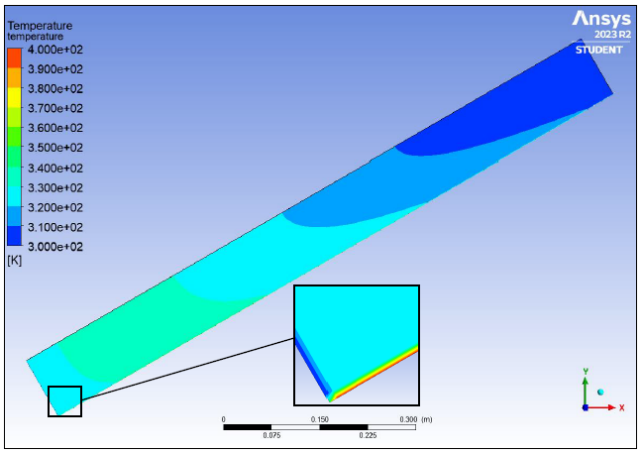

Figure 21: Temperature distribution

4 Conclusion

This study considered radiation, inclined stretching plate and Richardson number. The PDEs were converted into ODEs via similarity transformation, and the numerical results were executed using the bvp4c function in MATLAB. These $f''(0)$, $-\theta'(0)$ and the velocity and temperature profiles behavior are determined by taking into account N, Ri, Pr and various plate position. Thus, the following is a list of the findings in summary:

- As radiation increases, the values of $f''(0)$ increase while $-\theta'(0)$ decreases, indicating less resistance to fluid motion along the surface and higher surface temperatures.
- As the Richardson number increases, both $f''(0)$ and $-\theta'(0)$ are generally elevated due to stronger buoyancy-driven effects.
- The angle of inclination affects this velocity increase, with steeper angles usually resulting in higher velocities. Additionally, an inclined plate alters flow characteristics, which may reduce flow separation near the surface.
- CFD simulation results show that the fluid velocity is highest at the plate's surface but decreases as it moves away toward the free stream. This occurs because the fluid moves faster at the plate surface than in the surrounding area, following the Sakiadis flow boundary condition, in which the surface velocity is significant while the surrounding velocity equal to zero. The plate's surface temperature reaches its peak and progressively decreases as it nears the free stream. Likewise, the pressure at the inlet edge of the plate is at its minimum and steadily rises toward the free stream.

References

[1] Sakiadis, B. C. Boundary-layer behavior on continuous solid surfaces: I. Boundary-layer equations for two-dimensional and axisymmetric flow. *AIChE Journal*. 1961. 7(1), 26-28.

[2] Bataller, R. C. Numerical comparisons of Blasius and Sakiadis flows.*Matematika*. 2010. 187-196.

[3] Cortell, R. Flow and heat transfer of an electrically conducting fluid of second grade over a stretching sheet subject to suction and to a transverse magnetic field. *International Journal of Heat and Mass Transfer* 2006. 49(11–12), 1851-1856.

[4] Grubka, L. J., & Bobba, K. M. Heat transfer characteristics of a continuous stretching surface with variable temperature. *Journal of Heat Transfer*. 1985. 107(1), 248-250.

[5] Soid, S. K., & Ishak, A. Thermal boundary layer flow on a stretching plate with radiation effect. *2011 International Conference on Business, Engineering and Industrial Applications*. 2011. 120-124. IEEE.

[6] Ghasemi, S. E., & Hatami, M. Solar radiation effects on MHD stagnation point flow and heat transfer of a nanofluid over a stretching sheet. *Case Studies in Thermal Engineering*. 2021. 25, 100898.

[7] Dehsara, M., Habibi Matin, M., & Dalir, N. Entropy analysis for MHD flow over a non-linear stretching inclined transparent plate embedded in a porous medium due to solar radiation. *Mechanika*. 2012. 18(5), 524-533.

[8] Hayat, T., Asad, S., & Alsaedi, A. Flow of variable thermal conductivity fluid due to inclined stretching cylinder with viscous dissipation and thermal radiation. *Applied Mathematics and Mechanics (English Edition)*. 2014. 35(6), 717-728.

[9] Noor, N. A. M., Shafie, S., & Admon, M. A. Unsteady MHD flow of cassonnano fluid with chemical reaction, thermal radiation and heat generation/absorption.*Matematika*. 2019. 33-52.

[10] Izani, Siti Nur Haseela, and Anati Ali. "Thermal radiation effects on heat and mass transfer of magnetohydrodynamics dusty Jeffrey fluid past an exponentially stretching sheet.*Matematika*.2019. 187-200.

[11] Mishra, J., & Samantara, T. Study of Unsteady Two-Phase Flow over An Inclined Permeable Stretching Sheet with Effects of Electrification and Radiation. *Journal of Advanced Research in Fluid Mechanics and Thermal Sciences*. 2022. 97(2), 26-38.

[12] Siddiqa, S., & Hossain, M. A. Mixed convection boundary layer flow over a vertical flat plate with radiative heat transfer. 2012.

[13] Ghadikolaei, S. S., Hosseinzadeh, K., Yassari, M., Sadeghi, H., & Ganji, D. D. Analytical and numerical solution of non-Newtonian second-grade fluid flow on a stretching sheet. *Thermal Science and Engineering Progress*. 2018. 5, 309-316.

[14] Chaudhary, S., Chaudhary, S., & Singh, S. Heat Transfer in Hydromagnetic Flow over an Unsteady Stretching Permeable Sheet. *International Journal of Mathematical, Engineering and Management Sciences*. 2019. 4(4), 1018.

[15] Nandeppanavar, Mahantesh M., R. Madhusudhan, Achala L. Nargund, S. B. Sathyanarayana, and M. C. Kemparaju. "Application of HAM to laminar boundary layer flow over a wedge with an external magnetic field.*Heat Transfer*. 2022. 51(1), 170-192.

[16] Amar, N. Viscous dissipation and heat transfer effect on MHD boundary layer flow past a wedge of nano fluid embedded in a porous media.*Turkish Journal of Computer and Mathematics Education (TURCOMAT)*. 2021. 12(4), 1352-1366.

[17] Jabeen, K., Mushtaq, M., & Naeem, S. Role of suction/injection with magnetic dipole and double diffusion on nonlinear radiative Eyring-Powell nanofluid. Proceedings of the Institution of Mechanical Engineers, Part E: *Journal of Process Mechanical Engineering*. 2023. 09544089231162715.

[18] Norzawary, N. H. A., Soid, S. K., Ishak, A., Mohamed, M. K. A., Khan, U., Sherif, E. S. M., & Pop, I. Stability analysis for heat transfer flow in micropolar hybrid nanofluids.x*Journal of Process Mechanical Engineering*. 2023.5(20), 5627-5640.

[19] Norzawary, N. H. A., & Bachok, N. Slip Flow Via Nonlinearly Stretching/Shrinking Sheet in A Carbon Nanotubes.x*Journal of Process Mechanical Engineering*. 2023. 14(1), 8-19.

[20] Balamurugan, R., & Vanav Kumar, A. Mixed convection of transient MHD stagnation point flow over a stretching sheet with quadratic convection and thermal radiation.*Heat Transfer*. 2024.53(2), 584-609.

[21] Alzu'bi, O. A. S., Qabaah, A. S., Al Faqih, F. M., Yaseen, N., Shawaqfeh, S. A. M., & Swalmeh, M. Z. Newtonian heating on Casson mixed convection transport by ternary hybrid nanofluids over vertical stretching sheet: Numerical study. *Journal of Advanced Research in Fluid Mechanics and Thermal Sciences*. 2024. 115(1), 166-180.

[22] Mandal, B., Bhattacharyya, K., Banerjee, A., Kumar Verma, A., & Kumar Gautam, A. MHD mixed convection on an inclined stretching plate in Darcy porous medium with Soret effect and variable surface conditions. *Nonlinear Engineering*. 2020. 9(1), 457-469.

[23] Ganji, D. D., & Kachapi, S. H. H. Chapter 6-Natural, Mixed, and Forced Convection in Nanofluid. *Application of Nonlinear Systems in Nanomechanics and Nanofluids, DD Ganji and SHH Kachapi, Eds., in Micro and Nano Technologies., Oxford: William Andrew Publishing*. 2015. 205-269.

[24] Al-Sumaily, G. F., Dhahad, H. A., & Thompson, M. C. Mixed convection phenomenon in packed beds: A comprehensive review. *Thermal Science and Engineering Progress*. 2022. 32, 101242.

[25] Alabdulhadi, S., Waini, I., Ahmed, S. E., & Ishak, A. M. Hybrid nanofluid flow and heat transfer past an inclined surface. *Mathematics*. 2021. 9(24), 3176.

[26] Hamad, N. H., Bilal, M., Ali, A., Eldin, S. M., Sharaf, M., & Rahman, M. U. Energy transfer through third-grade fluid flow across an inclined stretching sheet subject to thermal radiation and Lorentz force. *Scientific Reports*. 2023. 13(1), 19643.

[27] Malik, H. T., Farooq, M., Ahmad, S., & Mohamed, M. M. I. Convective heat transportation in exponentially stratified Casson fluid flow over an inclined sheet with viscous dissipation. *Case Studies in Thermal Engineering*. 2023. 52, 103720.

[28] Norton, T., & Sun, D. W. Computational fluid dynamics (CFD) - An effective and efficient design and analysis tool for the food industry: A review.*Trends in Food Science & Technology*. 2006.17(11), 600-620.

[29] Murayama, Y., Fujimura, S., Suzuki, T., & Takao, H. Computational fluid dynamics as a risk assessment tool for aneurysm rupture. *Neurosurgical focus*. 2019. 47(1), E12.

[30] Dobhal, S., & Gupta, S. Numerical Study of Turbulence Models on Boundary Layer Flow over a Flat Plate using Computational Fluid Dynamics. *Journal of Adv Research in Applied Mechanics and Computational Fluid Dynamics*. 2020. 7(1).

[31] Mahdavi, M., Sharifpur, M., Ahmadi, M. H., & Meyer, J. P. Nanofluid flow and shear layers between two parallel plates: a simulation approach.*Engineering Applications of Computational Fluid Mechanics*. 2020. 14(1), 1536-1545.

[32] Alhamid, J., & Al-Obaidi, A. R. Effect of concavity configuration parameters on hydrodynamic and thermal performance in 3D circular pipe using Al2O3 nanofluid based on CFD simulation. In *Journal of Physics: Conference Series*. 2021. (Vol. 1845, No. 1, p. 012060). IOP Publishing.

[33] Algaidy, N., & Shrif A. E., Numerical simulation of the laminar boundary layer flow over a flat plate. *Journal of Alasmarya University: Applied Sciences*. 2023. 8(4), 122-135.

[34] Klazly, M. M. A., & Bognár, G. Computational fluid dynamic simulation of laminar flow over a flat plate. *Design of Machines and Structures*. 2019. 9(1), 29-47.